

Tutorial

Gassmann fluid substitutions: A tutorial

Tad M. Smith*, Carl H. Sondergeld†, and Chandra S. Rai‡

ABSTRACT

Fluid substitution is an important part of seismic attribute work, because it provides the interpreter with a tool for modeling and quantifying the various fluid scenarios which might give rise to an observed amplitude variation with offset (AVO) or 4D response. The most commonly used technique for doing this involves the application of Gassmann's equations.

Modeling the changes from one fluid type to another requires that the effects of the starting fluid first be removed prior to modeling the new fluid. In practice, the rock is drained of its initial pore fluid, and the moduli (bulk and shear) and bulk density of the porous frame are calculated. Once the porous frame properties are properly determined, the rock is saturated with the new

pore fluid, and the new effective bulk modulus and density are calculated.

A direct result of Gassmann's equations is that the shear modulus for an isotropic material is independent of pore fluid, and therefore remains constant during the fluid substitution process. In the case of disconnected or cracklike pores, however, this assumption may be violated. Once the values for the new effective bulk modulus and bulk density are calculated, it is possible to calculate the compressional and shear velocities for the new fluid conditions.

There are other approaches to fluid substitution (empirical and heuristic) which avoid the porous frame calculations but, as described in this tutorial, often do not yield reliable results. This tutorial provides the reader with a recipe for performing fluid substitutions, as well as insight into why and when the approach may fail.

INTRODUCTION

Fluid substitutions are an important part of any seismic attribute study, as they provide the interpreter with a valuable tool for modeling various fluid scenarios which might explain an observed amplitude variation with offset (AVO) anomaly. A common empirical approach for modeling velocity-porosity relationships was proposed by Wyllie et al. (1956, 1958) and later modified by Raymer et al. (1980). The most commonly used (and theoretically sound) approach at seismic frequencies is based on the work of Gassmann (1951), which relates the bulk modulus of a rock to its pore, frame, and fluid properties.

Unfortunately, many users of Gassmann's theory never develop an understanding of the strengths and weaknesses of the model, simply because of the widespread reliance on commercially available software. The purpose of this tutorial is to guide the reader through practical Gassmann fluid substitution, and

to highlight some of the commonly encountered caveats and pitfalls inherent to the modeling process. By understanding the equations and processes discussed in this tutorial, the reader should be able to program a spreadsheet or build a user program to perform fluid substitutions on a routine basis. We also include a simple case study from the deepwater Gulf of Mexico, using wireline log data.

As with any technology, recognition of pitfalls and the ability to diagnose and solve difficult problems comes with time and experience. Consequently, care should always be exercised when performing fluid substitutions, and experienced users should be consulted.

BACKGROUND

Modeling the effects of mineral composition, porosity, and fluid on seismic velocities is generally based on a combination

Manuscript received by the Editor October 18, 2001; revised manuscript received October 1, 2002.

*Formerly Veritas DGC, Houston, Texas; presently Newfield Exploration, 363 North Sam Houston Parkway E., Houston, Texas 77060. E-mail: tmsmith@newfld.com.

†University of Oklahoma, 4502 E. 41st Street, Tulsa, Oklahoma 74135. E-mail: csondergeld@ou.edu.

© 2003 Society of Exploration Geophysicists. All rights reserved.

of empirical relationships and theoretical formulations. Empirical approaches attempt to establish relationships between porosity, fluid velocities, and the velocity of the rock matrix, and generally involve regression analyses of core or log measurements (e.g., Wyllie et al., 1956; Raymer et al., 1980; Han et al., 1986; Eberhart-Phillips et al., 1989). However, these relationships are not based on physical principles and generally do not work well for fluid substitution modeling.

The most commonly used theoretical approach for fluid substitutions employs the low-frequency Gassmann theory (Gassmann, 1951). Gassmann's equation relates the saturated bulk modulus of the rock to its porosity, the bulk modulus of the porous rock frame, the bulk modulus of the mineral matrix, and the bulk modulus of the pore-filling fluids:

$$K_{sat} = K^* + \frac{\left(1 - \frac{K^*}{K_o}\right)^2}{\frac{\phi}{K_{fl}} + \frac{(1-\phi)}{K_o} - \frac{K^*}{K_o^2}}, \quad (1)$$

where K_{sat} = the saturated bulk modulus (undrained of pore fluids), K_o = the bulk modulus of the mineral matrix, K_{fl} = the bulk modulus of the pore fluid, K^* = the bulk modulus of the porous rock frame, (drained of any pore-filling fluid), and ϕ = porosity.

Application of this equation is a two-part process, whereby we first determine the bulk modulus of the porous rock frame (the bulk modulus of the rock drained of its initial pore-filling fluid, also referred to as the "dry frame" bulk modulus), after which we calculate the bulk modulus of the rock saturated with any desired fluid.

When applying equation (1) to core measurements, it is important to recognize that the "dry frame" bulk modulus, K^* , represents the "dry frame" property of the rock with a small amount of moisture present (see Clark, et al., 1980). In practice, these values would come from controlled humidity-dried core samples. Predicted velocities will be too fast if the porous rock frame is assumed to be absolutely dry. In this tutorial, rather than confuse the reader by referring to the "dry frame" properties, we instead refer to the "porous rock frame".

Model assumptions

Application of Gassmann's equation is based on several assumptions. First, the model assumes that the rock is homogeneous and isotropic, and that the pore space is completely connected. This assumption is violated if the rock framework is composed of multiple minerals with large contrasts in elastic stiffness (Berge, 1998), or if it composed of preferentially-oriented anisotropic minerals (Brown and Korringa, 1975). Fortunately, Gassmann's equation is free of assumptions about pore geometry, although the pore system must be connected and fluids must be moveable. However, when multiple pore types are present in a rock, it is often necessary to use more complex models (Berryman and Milton, 1991; O'Connell, 1984; Berryman and Wang, 2000). Note that many of the assumptions regarding pore connectivity and pore type are probably violated in low-porosity rocks. Carbonate rocks, in particular, may be problematic due to the diverse pore types often observed in thin section and the low connectivity of these pores.

Second, Gassmann's equation is valid only at low enough frequencies such that pore pressures are equalized over a length scale much greater than a pore dimension and much less than the wavelength of the passing seismic wave. For high frequencies, original formulations presented by Biot (1956, 1962) should be used. At sonic logging frequencies, Gassmann may or may not be applicable (Berryman, 1999), although reliable results are often obtained for clean sands with high effective porosities, such as those encountered in the deepwater Gulf of Mexico. Unreliable results often occur when applying Gassmann's equation to low-porosity or shaly sands or to carbonate rocks. This is because basic assumptions regarding frequency or pore connectivity are violated.

In this tutorial, we focus on simple application of equation (1) and assume that all the model assumptions are met. Additional pitfalls and sources of error are discussed in a later section.

DEFINITIONS

Prior to delving into Gassmann, we must first define and briefly discuss the bulk and shear moduli of the rock, as well as the bulk modulus of the pore-filling fluid. In addition, we must also discuss techniques for mixing complex mineralogies and multiple fluids. For excellent and comprehensive reviews of rock and fluid properties, the reader is referred to Batzle and Wang (1992), Castagna et al. (1993), Mavko et al. (1998), and Wang (2001).

Rock properties

Gassmann's equation relates the saturated bulk modulus of the rock (K_{sat}) to its porous frame properties and the properties of the pore-filling fluid [equation (1)]. The bulk modulus, or incompressibility, of an isotropic rock is defined as the ratio of hydrostatic stress to volumetric strain. Values for bulk modulus can be obtained either by dynamic laboratory measurements of velocities or from analysis of wireline log data (typical static measurements for the moduli violate the assumption of infinitesimal strain, and should be avoided for fluid substitution purposes). Whether from dynamic velocity measurements or from wireline log data, we can relate the bulk modulus of a rock, K_{sat} , to its compressional velocity, shear velocity, and bulk density through the following relationship:

$$K = \rho_B \left(V_p^2 - \frac{4}{3} V_s^2 \right), \quad (2)$$

where ρ_B is the bulk density of the rock, V_p is its compressional velocity, and V_s is its shear velocity. Note that this equation is easily rewritten and solved for V_p . If velocity and density measurements are used to calculate K_{sat} from wireline log data, the resulting value will be the bulk modulus of the rock saturated with the in-situ pore fluid. If velocity measurements are made on controlled humidity-dried core samples, the calculated bulk modulus will represent the bulk modulus of the porous rock framework, K^* .

The shear modulus (G), or shear stiffness, of a rock is defined as the ratio of shear stress to shear strain. As with the bulk modulus, it can be determined by laboratory tests or analysis of wireline log data, and is given by the following equation:

$$G = \rho_B V_s^2. \quad (3)$$

The shear modulus, G , is also frequently represented by the symbol μ .

If velocities are in kilometers per second and densities are in grams per cubic centimeter, the resultant moduli (K and G) will be in gigapascals (GPa). It is important to recognize that the saturated bulk modulus of a rock may be sensitive to the composition of the pore-filling fluid, whereas the shear modulus is insensitive to pore fluid [that is, $G_{dry} = G_{wet}$ (Biot, 1956; Berryman and Milton, 1991; Berryman, 1999)]. Thus, the shear modulus does not vary during the course of a fluid substitution. This understanding is fundamental to application of Biot-Gassmann theory in general, and Gassmann's equation specifically.

A fourth equation is also necessary for performing fluid substitutions. This equation describes the relationship between the fluid density (ρ_f), porosity (ϕ), grain density of the rock matrix (ρ_g), and the rock bulk density (ρ_B):

$$\rho_B = \rho_g(1 - \phi) + \rho_f\phi. \quad (4)$$

This equation is also easily rewritten and solved for porosity.

USING GASSMANN'S EQUATION

Before we begin fluid substitution using equation (1), we must first determine (1) the porosity of the rock, ϕ , (2) the properties of the fluids (K_f , ρ_f) that occupy the pore space, (3) the bulk modulus of the mineral matrix (K_0), and (4) the bulk modulus of the porous rock frame (K^*). All four components may be defined or inferred through laboratory measurement or analysis of wireline log data.

Porosity

Porosity is routinely calculated from core data or from analysis of wireline log data [equation (4)] is rewritten and solved for porosity. Because logging tools do not directly measure porosity or bulk density, calibration of the log-derived porosity to measured core porosity is highly desirable, and in some instances (e.g., when dealing with complex lithologies or low-porosity rocks) may significantly alter the results of a fluid substitution. Core calibration may also be particularly important if the formation is invaded by drilling fluids.

Fluid properties

Prior to performing a fluid substitution, we must also know something about the bulk modulus and density of the in-situ pore-filling fluid, as well as those of the new fluid we wish to model. Three approaches are commonly used for determining these values: (1) the properties are measured directly (at reservoir temperatures and pressures) from pore fluids recovered from the reservoir, (2) the properties are calculated from equations of state (see McCain, 1990; Danesh, 1998), or (3) the properties are calculated from an empirical calculator (e.g., Batzle and Wang, 1992). Note that typical laboratory analyses of reservoir fluids yield the isothermal properties of the fluid bulk modulus, whereas wave propagation involves the adiabatic properties. Generally, the difference between the two is small unless the fluid has a relatively high gas-oil-ratio (GOR). For additional detailed information on the behavior of fluids, the reader is referred to McCain (1990), Batzle and Wang (1992), and Danesh (1998).

Because there typically are two or more fluid phases occupying the pore space of a reservoir rock, we must calculate a bulk modulus and density of the individual fluid end members, and then mix the fluids according to the following physical rules. Gassmann's equation assumes all the pore space is connected and pore pressure is equilibrated throughout the rock. Thus, the assumptions of a homogeneous fluid, uniformly distributed throughout the pore space, allows the bulk modulus of the fluid mixture to be calculated via the isostress, or Reuss, average:

$$K_f = \left[\sum_{i=1}^n \frac{S_i}{K_i} \right]^{-1}, \quad (5)$$

where K_f is the bulk modulus of the fluid mixture, K_i is the bulk modulus of the individual phases, and S_i is their saturation. For a simple two-component hydrocarbon-water system, this equation becomes

$$K_f = \left[\frac{S_w}{K_w} + \frac{(1 - S_w)}{K_{hc}} \right]^{-1}, \quad (6)$$

where S_w is the water saturation, K_w is the bulk modulus of the water, and K_{hc} is the bulk modulus of the hydrocarbon. This equation is easily expanded to account for additional fluid phases.

For the fluid density, a simple volumetric mix of the end-member components is used to calculate the density of the fluid mixture:

$$\rho_f = \sum_{i=1}^n S_i \rho_i, \quad (7)$$

where S_i is the saturation of the individual components, and ρ_i is the density of the individual components. For a simple two-component hydrocarbon-water system, this equation becomes:

$$\rho_f = S_w \rho_w + (1 - S_w) \rho_{hc}, \quad (8)$$

where ρ_w is the density of water, and ρ_{hc} is the density of the hydrocarbon. As with equation (6), this equation is easily expanded to include additional fluid phases.

Matrix properties

To calculate the bulk modulus of the mineral matrix, K_0 , information on the composition of the rock must be available. If core samples are available, mineral abundance may be determined using conventional laboratory techniques [e.g., point counting of thin sections, X-ray diffraction, or Fourier transform infrared analysis (Sondergeld and Rai, 1993)]. In the absence of core data, lithology can be approximated from wireline logs by simple clay volume (V_{clay}) analysis and assuming the two mineral end members are quartz and clay. For more complex lithologies, however, other techniques must be applied which allow the volumetric abundance of the mineral constituents to be estimated (e.g., deterministic techniques, multilinear regression, neural networks, etc.).

Once the mineral abundances are determined, K_0 is calculated via application of Voigt-Reuss-Hill (VRH) averaging of the mineral constituents [alternatively, Hashin-Shtrikman (HS) averaging may be used (Hashin and Shtrikman, 1962)]. A VRH average is simply the average of the harmonic (Reuss average) and arithmetic means (Voigt average) for the mineral constituents (Figure 1). If compliant minerals are located

at grain contacts, it may be more appropriate to use a simple Reuss average when calculating K_0 .

For a simple rock consisting of two minerals, this can be expressed as

$$K_{Reuss} = \left[\frac{F_1}{K_1} + \frac{F_2}{K_2} \right]^{-1}, \quad (9)$$

$$K_{Voigt} = [F_1 K_1 + F_2 K_2], \quad (10)$$

$$K_{vrh} = \frac{1}{2}[K_{Voigt} + K_{Reuss}], \quad (11)$$

where F_1 and F_2 are the volumetric fractions of the two components, and K_1 and K_2 are the bulk moduli of the two components. Note that these equations may be readily expanded to include additional mineral components. Values for the bulk moduli of the most common sedimentary minerals are included in Table 1. See Carmichael (1989) for a more comprehensive list of seismic rock properties.

Frame properties

Prior to applying Gassmann's equation, it is necessary to determine the bulk modulus of the porous rock frame, K^* . This is the low-frequency, drained bulk modulus of the rock. Once determined, K^* is held constant during the course of a fluid substitution. Note that the shear modulus, G [(equation (3)], is also a frame property of the rock and is therefore also held constant during the typical fluid substitution process.

K^* may be derived either from (1) velocity measurements on controlled humidity-dried core, (2) application of empirical relationships or effective medium theory (Budiansky and O'Connell, 1976; Gregory, 1976; Murphy et al., 1993; Spencer et al., 1994; Vernik, 1998; Wang, 2000, 2001), or (3) direct calculation from log data (Zhu and McMechan, 1990). When working with core data, it is important to recognize that velocities

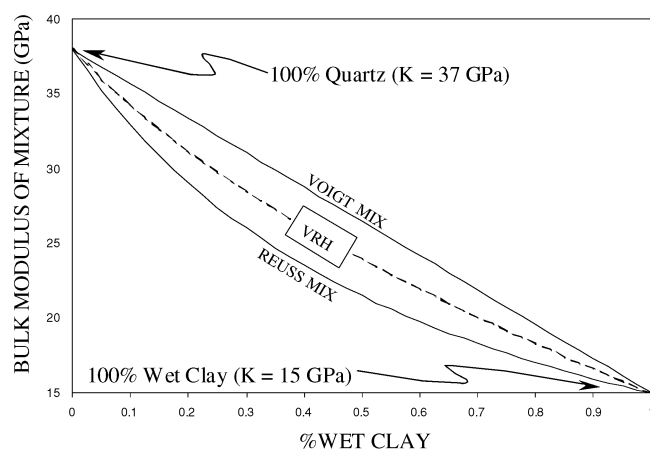


FIG. 1. Matrix properties are often calculated using a VRH-average, which is simply the average of the Reuss [equation (9) and Voigt equation (10)] averages of individual mineral end-member components. In this diagram, we mix pure quartz with wet clay. The Voight mix is the “stiff” upper bound, whereas the Reuss mix is the “weak” lower bound. The VRH average is simply the average of the Voigt and Reuss bounds. The VRH mixing scheme is used to determine the matrix bulk modulus of the rock (i.e., the bulk modulus of the minerals with no effective porosity present).

computed from completely dry samples will be too high. This is because the first few monolayers of water chemically weaken the rock (Clark et al., 1980). Thus, it is this slightly wet, or drained, measurement of K^* which should be used when performing Gassmann fluid substitutions on core data.

When working with wireline log data, one common approach for determining K^* is to rewrite equation (1) such that (Zhu and McMechan, 1990)

$$K^* = \frac{K_{sat} \left(\frac{\phi K_o}{K_{fl}} + 1 - \phi \right) - K_o}{\frac{\phi K_o}{K_{fl}} + \frac{K_{sat}}{K_o} - 1 - \phi}. \quad (12)$$

Thus, the saturated bulk modulus of the rock (K_{sat}) for the in-situ conditions is first calculated using equation (2), and the other terms (K_{fl} , K_o , and ϕ) are calculated using the processes described above. For purposes of calculating K^* , K_{fl} is the bulk modulus of the pore-filling fluids under in-situ conditions. Note that uncertainties in porosity, water saturation, fluid properties, or lithology will lead to errors in the calculated value of K^* .

Since porosity appears explicitly in equations (1) and (12), it is tempting to use these equations to model porosity-velocity relationships. Note, however, that the value of K^* depends, in part, upon the porosity of the rock. Thus, porosity modeling can only be accomplished if a relationship can be established between the porous frame properties of the rock and porosity (c.f., Budiansky and O'Connell, 1976; Murphy et al., 1993). Thus, it is incorrect to use equations (1) and (12) for porosity modeling without properly adjusting K^* .

CALCULATING VELOCITIES

Assume we have calculated porosity (ϕ) along with the matrix and frame properties of the rock (K_0 , K^* , and G). This allows us to use equation (1) to calculate a new saturated bulk modulus for any desired fluid [the bulk modulus of a fluid can be calculated using equation (5)].

Next, we must use equations (4) and (7) to calculate a new bulk density for the rock. Once the new bulk density of the rock

Table 1. Bulk modulus, shear modulus, and bulk density of common rock forming minerals.* Values are from Carmichael (1989).

Mineral	Bulk Modulus (GPa)	Shear Modulus (GPa)	Density (g/cm ³)
Quartz	37	44	2.65
“Average” feldspar	37.5	15	2.62
Plagioclase feldspar	75.6	25.6	2.63
clay	variable	variable	variable
Pyrite	147.4	132.5	4.93
Hematite	100.2	95.2	5.24
Calcite	76.8	32	2.71
Dolomite	94.9	45	2.87
Siderite	123.7	51	3.96
Anydrite	44.8	29.1	2.98

*Note that the bulk modulus of clay minerals are highly variable. For more information on clay properties, see Wang et al., 2001.

is calculated, we can rewrite equation (2) and calculate V_p :

$$V_p = \sqrt{\frac{K_{sat} + \frac{4}{3}G}{\rho_B}}. \quad (13)$$

We also rewrite equation (3) and use the new bulk density to calculate the new shear velocity:

$$V_s = \sqrt{\frac{G}{\rho_B}}. \quad (14)$$

Since the shear modulus, G , is held constant during the course of a fluid substitution, we see from equation (14) that the shear velocity of a gas sand will be faster than the shear velocity of a brine sand. A summary workflow for Gassmann fluid substitutions is included in Table 2.

CAVEATS AND PITFALLS

As with all models, certain assumptions are made during the fluid substitution process (discussed earlier). Failure to understand these assumptions, or simple application of the wrong assumptions, can lead to unrealistic and potentially costly answers. In this section, we review some of the additional pitfalls and that may lead to incorrect models.

Invasion effects

When processing log data for seismic modeling, it is important to evaluate the log response for the effects of invasion (Alberty, 1994; Walls and Carr, 2001). Because water saturations are typically computed from a deep resistivity device (which looks several feet into the formation), calculated S_w values most likely do not reflect the saturation seen by the sonic and density logs, which have much shallower depths of investigation. Thus, it may be necessary to apply invasion corrections to the sonic and density response, if possible.

Invasion corrections require accurate estimates of water saturation in the invaded zone (S_{xo}), as well as accurate estimates of porosity. In addition, knowledge of the mud and formation fluid properties (K and ρ) is necessary. If these data are available or can be reasonably estimated, it is possible to use equation (4) and Gassmann's equation [Equation (1)] to correct

Table 2. Workflow for application of Gassmann's equation.

-
1. Log edits and interpretation.
 2. Shear velocity estimation (if necessary).
 3. Calculate K and G for the in-situ conditions [equations (2) and (3)].
 4. Calculate K_0 based on lithology estimates [VRH or HS mixing; equations (9)–(11)].
 5. Calculate fluid properties (K and ρ).
 6. Mix fluids for the in-situ case according to S_w [equations (5) and (7)].
 7. Calculate K^* [equation (12)].
 8. Calculate new fluid properties (K and ρ) at the desired S_w [equations (5) and (7)].
 9. Calculate the new saturated bulk modulus of the rock using Gassmann [equation (1)].
 10. Calculate the new bulk density [equation (4)].
 11. Calculate the new compressional velocity [equation (13)].
 12. Calculate the new shear velocity [equation (14)].
-

rect the log data. If homogeneous saturations are assumed, the changes to the sonic data will be small (unless $S_{xo} > \sim 90\%$). Sonic corrections may be larger if patchy saturation is assumed (Endres and Knight, 1989; Packwood and Mavko, 1995), or if gas is unevenly distributed among pores of different shapes (Knight and Nolen-Hoeksema, 1990; Castagna and Hooper, 2000).

Dry frame bulk modulus, K^*

Application of Gassmann's equation is dependent upon accurate determination of the porous frame properties of the rock (K^* and G). In order to calculate the shear modulus, G , it is only necessary to know the bulk density and shear velocity of the formation. However, in order to calculate the bulk modulus of the porous rock frame, certain assumptions must be made about the matrix and fluid properties (see previous discussion). Thus, K^* is interpretive, in part, and errors in either matrix or fluid properties will lead to errors in the calculated value for K^* . Indeed, in many cases with complex lithology, K^* may be negative (a physical impossibility) or unrealistically large. Sources of anomalous K^* values may be when (1) porosities or matrix properties are incorrect, (2) fluid properties are incorrect (McLean and Alberty, 2001), or (3) initial assessments of water saturation are incorrect. A technique we recommend for evaluating K^* is to compute the ratio of K^* to G . For clean sands, this ratio is usually close to 1 (Spencer et al., 1994; Wang, 2001), whereas for shaly sands it may approach 2–3. Theoretical models, as well as empirical observations, support this behavior (Budiansky and O'Connell, 1976; Nur et al., 1995; Wang, 2001) (Figure 2). Note that this approach may not work for sands with complex mineralogy or in carbonate rocks. Indeed, Ramamoorthy and Murphy (1998) show that the K^*/G ratio can vary substantially in carbonates.

Patchy saturation

A typical application of Gassmann's equation assumes that all fluid phases are immiscible and homogeneously distributed throughout the pore space (homogeneous saturation). These assumptions are thought (expected) to be satisfied in systems which have come to equilibrium over geologic time. However, this equilibrium distribution of phases may be disturbed during drilling, production, and water flooding, and the return to equilibrium may require time frames longer than those encountered during logging or between seismic surveys used in 4D monitoring. Thus, it is reasonable to expect that fluids might not be uniformly or homogeneously distributed throughout the pore space in a reservoir or borehole (Brie et al., 1995). Furthermore, in water-wet rock, water is preferentially drawn into the smaller size pores and cracks, leaving the larger voids or pores preferentially occupied by the hydrocarbons. This may lead to a segregation of phases and, perhaps more importantly, the inability of pore pressures to equilibrate in the time scale of wave propagation. Thus, conditions can and probably do exist where water and hydrocarbon distribution are not uniform and the application of the Reuss average for fluid mixture properties is inadequate. This class of nonuniform phase distributions is sometimes referred to as "patchy saturation," and can be modeled if the following assumptions are made: (1) the shear modulus does not vary as a function of pore fluid; (2) the fluids are

spatially distributed in aggregates whose dimensions are much smaller than the seismic wavelength; and (3) the different pore fluid “patches” have dimensions which do not allow fluid pressure equalization during the time scale of wave propagation. Hill (1963) and Berryman and Milton (1991) have developed the formalism for estimating the effective bulk modulus under these conditions:

$$K_{eff} = \left[\sum_{i=1}^n \frac{x_i}{\left(K_i + \frac{4}{3}G \right)} \right]^{-1} - \frac{4}{3}G, \quad (15)$$

where n = the number of patches with different fluid content, x_i = the volume fraction of the i th patch, G = the shear modulus of the rock, K_i = the bulk modulus of the rock completely saturated with the i th fluid, and K_{eff} = the effective bulk modulus of the rock.

Importantly, Hill (1963) demonstrated that equation (15) holds for general aggregates, where the shear modulus is the same for all constituents. In addition, the Backus (1962) average for isotropic layers having a constant shear modulus reduces to equation (15). Note that nonuniform saturation will have no effect on the calculated shear velocity, because the shear modulus of a rock is independent of the pore-filling fluid under the conditions discussed above. Incorporating nonuni-

form saturation into the Gassmann modeling allows us to continue to ignore the details of the pore geometry. However, microstructural details can exist which lead to preferential fluid segregation that can not be adequately modeled using either simple Gassmann or patchy saturation (e.g. Endres and Knight, 1989; Castagna and Hooper, 2000).

Figure 3 shows the effect of patchy (nonhomogeneous) saturation on a high-porosity (30%) sand and a lower-porosity sand (19%); both examples are from wireline log data. The percent difference between patchy and homogeneous saturation for both scenarios is shown in Figure 3c. For the lower-porosity sand case, the difference between patchy and homogeneous saturation is less than 5%, whereas the difference approaches 12% for the higher-porosity sand case (when S_w approaches ~80%). Clearly, it becomes important to consider the potential effects of patchy saturation for high-porosity sands (Figure 3b), although it will be most problematic for the case of low gas saturation ($S_w \approx 80\%$). Thus, consideration of nonuniform versus homogeneous saturation may become particularly important when applying invasion corrections to wireline log data and in modeling time-lapse seismic responses.

Internal consistency and saturation modeling

Fluid substitution models should always be carefully evaluated for quality and internal consistency. For instance, when

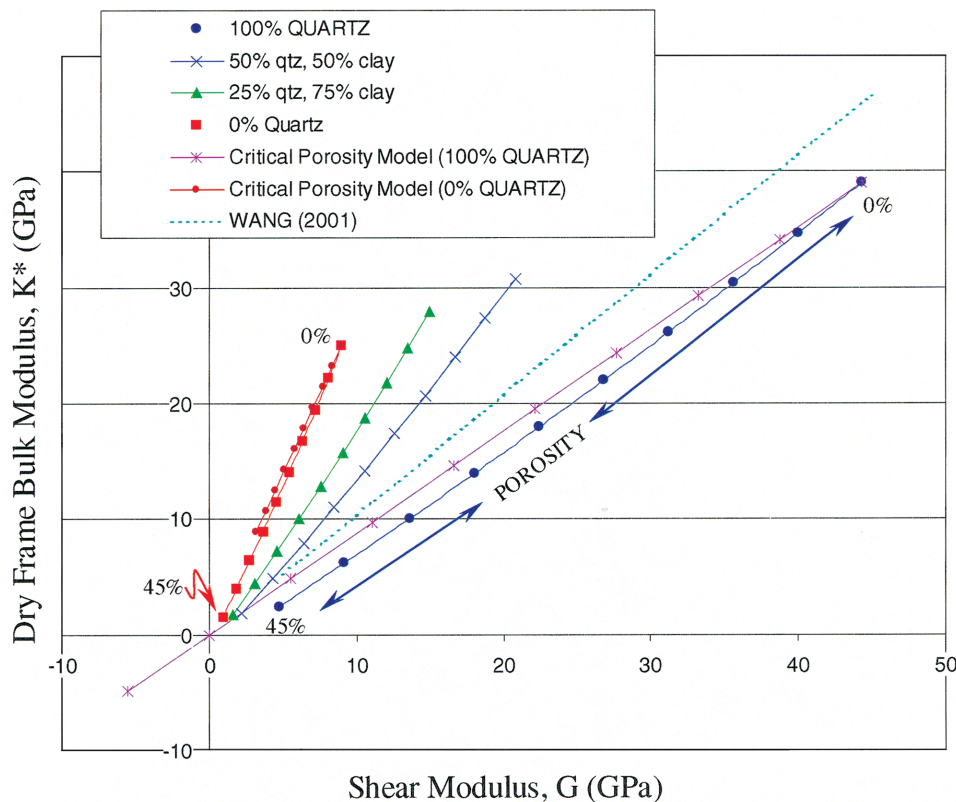


FIG. 2. Model-based and empirical relationships between the shear modulus, G , and the porous frame bulk modulus, K^* . The self-consistent models of Buijansky and O’Connell (1976) and the critical porosity models of Nur et al. (1995) yield similar results and suggest that K^*/G should be greater than 1 for shaly sands. The empirical result of Wang (2001) is also included for comparison. His data show that the K^*/G ratio should be approximately equal to 1. Note that for shaly sands and low porosity sands, many of the assumptions discussed in this tutorial are violated.

oil or gas is substituted into a brine sand, bulk densities should always decrease and shear velocities should always increase (assuming no adjustments were made to K^* , G , or porosity). If the expected changes in V_s or density are not observed to occur or if the magnitude of change is not what is expected, errors must exist in one or more of the input parameters. For density and shear velocity, these errors will most likely be in grain density or porosity.

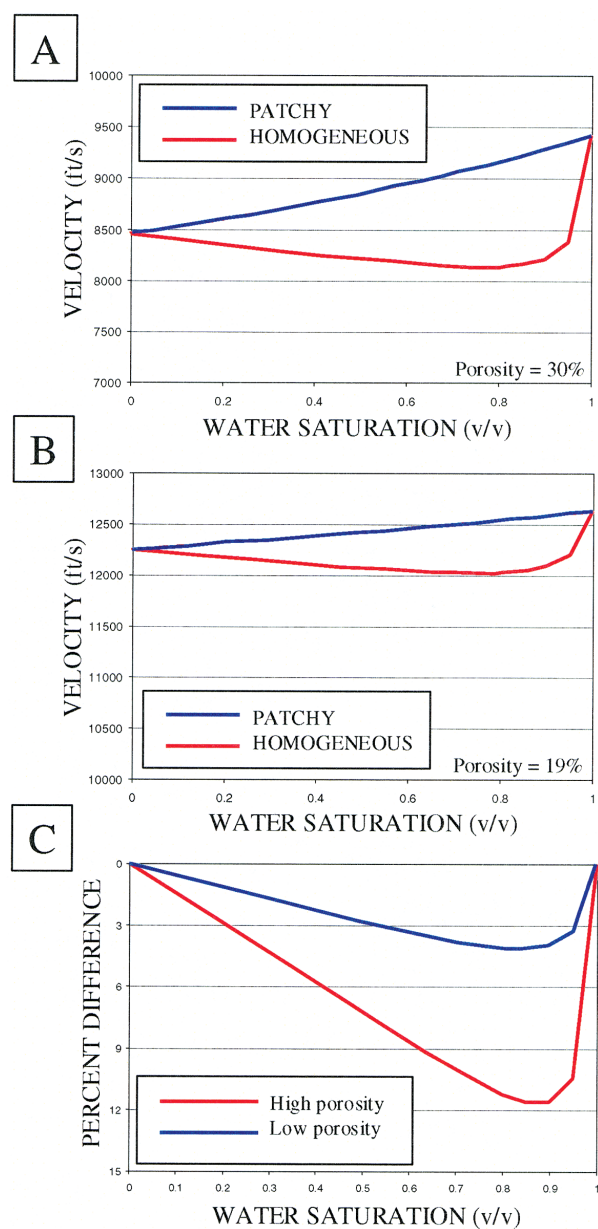


FIG. 3. Homogeneous versus nonhomogeneous saturation for a gas-brine system. (a) High-porosity sand, (b) low-porosity sand, and (c) percent difference plot. Both models are derived from wireline log data. Note from (c) that patchy saturation may be particularly problematic at low gas saturations ($S_w \approx 0.80$). Patchy saturation [or other dispersion mechanisms (Brie et al., 1995; Castagna and Hooper, 2000)] may also be important to consider when correcting wireline sonic logs for invasion.

To aid as a quality-control check on fluid substitutions and in order to best understand how velocities and densities should vary for any given sand, it is often instructive to generate saturation models, where Gassmann's relationships are used to calculate V_p , V_s , and ρ_B as a function of water saturation (Figure 4). These types of models are particularly important for understanding the rare case when compressional velocities for a gas sand are faster than those for oil in the same sand (Figure 4b). This situation can occur when the bulk density decreases at a faster rate than the saturated bulk modulus as gas saturation is increased.

CONVENTIONAL APPLICATION

Conventional application of Gassmann's equation provides the interpreter with a powerful tool for evaluating the various fluid scenarios which might give rise to an AVO anomaly (e.g., Sbar, 2000). In this paper, we use velocities and densities from a gas sand in a deepwater Gulf of Mexico well to illustrate conventional application of Gassmann's equation (Figure 5). Using the processes described in this paper, we replace the

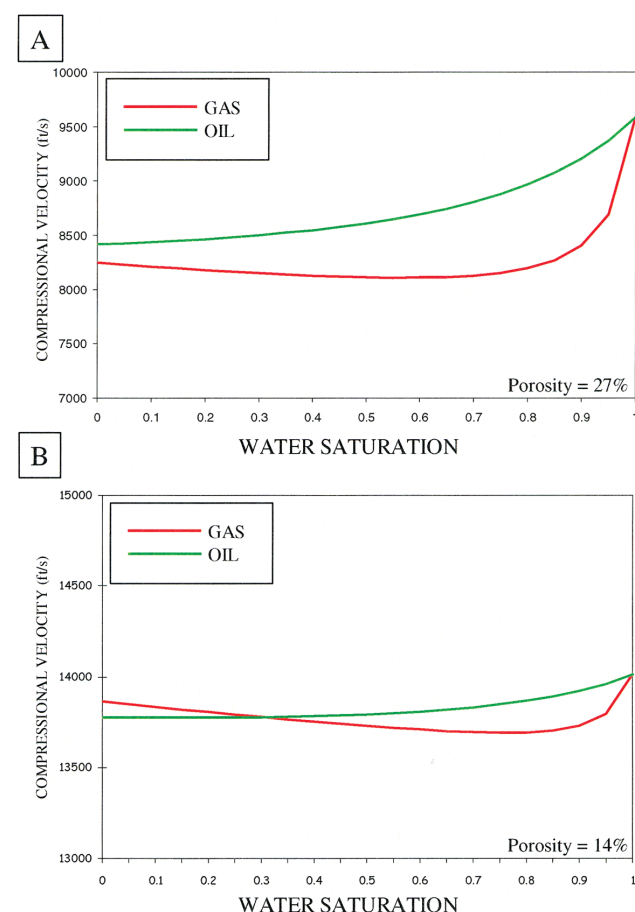


FIG. 4. Saturation models generated using Gassmann's equation. (a) High-porosity sand from the deepwater Gulf of Mexico, (b) low-porosity sand from South America. Note the small differences between the gas and oil case at low water saturations ($S_w < 0.30$). Also note from (b) that the gas sand velocity at low values of S_w is actually faster than the oil sand velocity.

in-situ gas with brine (Figure 5). Inferred fluid properties are included in Figure 5.

Large differences are observed in the density and compressional velocity response between gas and brine, whereas much smaller differences are observed in shear velocity. Note, however, that the shear velocity for gas is faster than the shear velocity for brine. Examination of equation (14) shows that this behavior is to be expected. Also note from this figure that the calculated porous frame bulk modulus [K^* , calculated using Equation (12)] is nearly equal in value to the shear modulus. This is to be expected for clean quartz sands.

In Figure 6, we cross-plot acoustic impedance and Poisson's ratio. We note from this that the brine sands and shale are

distinct from the gas response. In the analysis of actual seismic data, it is this deviation from the brine and shale "background" trend which will allow us to identify gas or oil anomalies (see Castagna and Swan, 1997). Construction of this type of crossplot from petrophysical data also allows us to quantify the difference between different fluid scenarios. It is also common to replace Poisson's ratio in these crossplots with elastic or shear impedance (Connolly, 1999; Vernik and Fisher, 2001).

Simple interface models are also constructed for this sand (Figure 7) using Shuey's three-term approximation (Shuey, 1985). Notice that the in-situ gas case generates a positive class III AVO response (negative gradient), whereas the brine

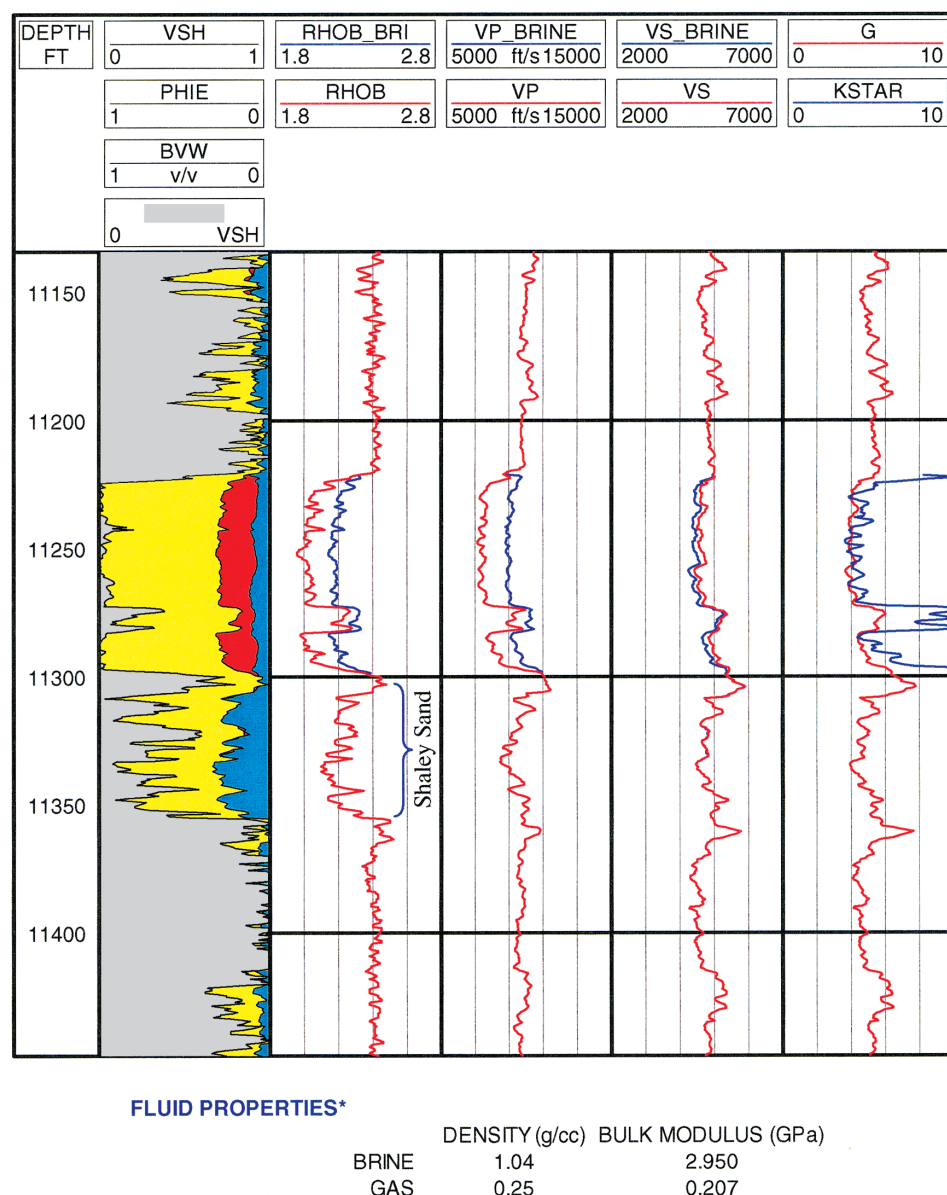


FIG. 5. Gas sand from a deepwater Gulf of Mexico well (water depth is approximately 1000 m). In relatively high-porosity rocks such as these, there is a large contrast between the gas and brine response. Also included in this plot are curves showing the shear modulus, G , and the dry frame bulk modulus, K^* . Note that K^* is nearly equal to G for sands with low clay contents, whereas it may be much higher than G for shaly sands.

case generates a negative AVO response (positive gradient). In both cases, large differences in intercept are observed.

The interface models shown in Figure 7 are derived from interval averages calculated from the log data, and therefore represent a single point reflection with infinite half-spaces above and below the reflector. This allows us to develop an understanding of the AVO response these rocks are capable of generating in the absence of complications resulting from sand thickness and geometry, seismic frequency, and the shape of the seismic wavelet. Unfortunately, the response calculated from these simple interface models is not always representative of the observed response. Thus, we must scale up our data to the seismic bandwidth for a direct comparison to seismic data.

Figure 8 is a comparison of the offset synthetic response for both gas and brine. For these models, a simple bandpass filter was applied with a frequency spectrum of 5–10–40–50 Hz. Note that the AVO response is still observed at the seismic bandwidth. Clearly, AVO (and other AVO-based attributes) could be used to help differentiate gas and brine for this particular example. Caution should always be used, however, when comparing these types of models to the actual seismic gathers, as improper processing of the seismic data can significantly alter the amplitude response of the data.

CONCLUSIONS

Gassmann's equations provide the seismic interpreter with a powerful framework for evaluating various fluid scenarios

which might give rise to an observed seismic anomaly. We have attempted in this tutorial to provide the reader with a practical understanding of the "nuts-and-bolts" behind conventional application of Gassmann. However, this technology is often perceived as being "black box," and is frequently applied via commercial software packages without much knowledge of how the calculations are being made or where the potential pitfalls may occur. In particular, invasion corrections and proper determination of the porous frame properties (in particular, K^*) are critical for generating internally consistent and meaningful results. Failure to be aware of these problems can, and frequently does, lead to models which are wrong. Once reliable models are obtained, the user can quantify the differences between the hydrocarbon and brine case by crossplot analysis, interface modeling, and offset synthetic analysis.

ACKNOWLEDGMENTS

The authors thank Bruce Wagner (BP Americas), Yafei Wu (VeritasDGC), and Dave Went (VeritasDGC) for early and critical reviews of the original manuscript. In addition, the quality of the manuscript was greatly improved by the comments from John Castagna, Yue Feng Sun, Enders A. Robinson, and two anonymous reviewers. The authors are particularly indebted to Keith Katahara (BP Americas) for several reviews of this manuscript and for numerous stimulating and enlightening discussions on fluid substitutions and seismic rock properties. Editorial support was provided by Harold Cansler (Petrophysical Solution) and Mandy Jones and Ken Williams (VeritasDGC).

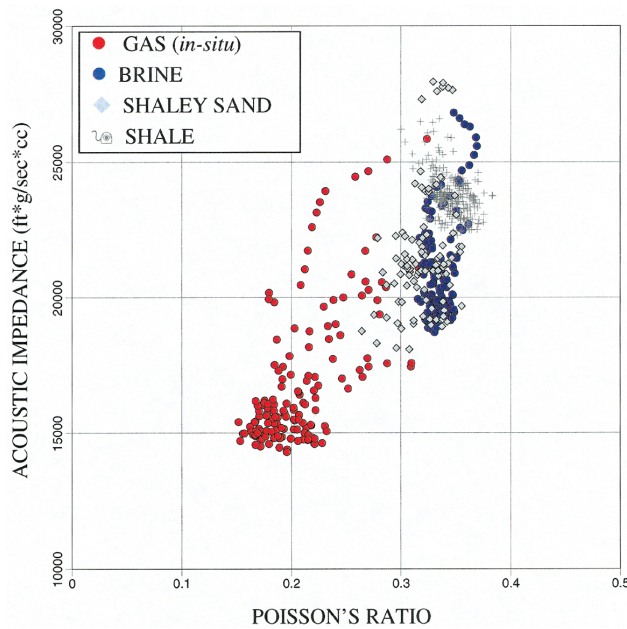
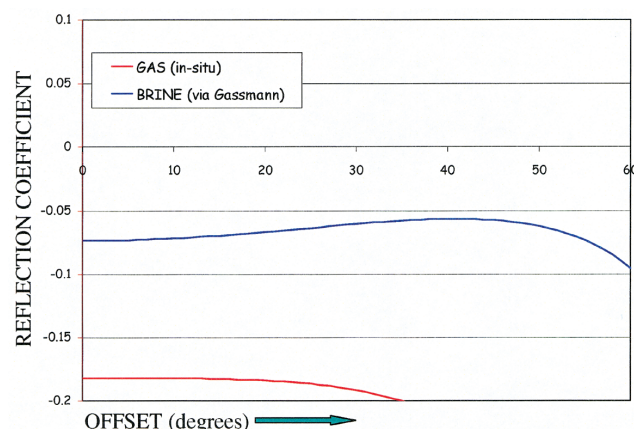


FIG. 6. Acoustic impedance versus Poisson ratio crossplot of the well data shown in Figure 5. Brine sands and shale can be used to define the "background" trend against which gas anomalies may be quantified (Castagna and Swan, 1997). The magnitude of deviation from the shale and brine sand "background" will be variable, and is largely dependent on rock type and quality. For low-porosity sands, small differences are typically observed between the "background" trend and the gas response.



INPUT PARAMETERS:

	SHALE	GAS (in-situ)	Brine
VP (ft/s)	9941	7969	9352
VS (ft/s)	4894	4798	4646
RHOB (g/cc)	2.41	2.08	2.21

FIG. 7. Interface models [Shuey's three-term approximation (Shuey, 1985)] for the sand shown in Figure 5. Note that large differences in intercept and gradient are observed between the gas and brine cases. The in-situ response is for gas, and is calculated using the measured velocities and density from wireline log data. The brine response is calculated using Gassmann's equation. RHOB = bulk density.

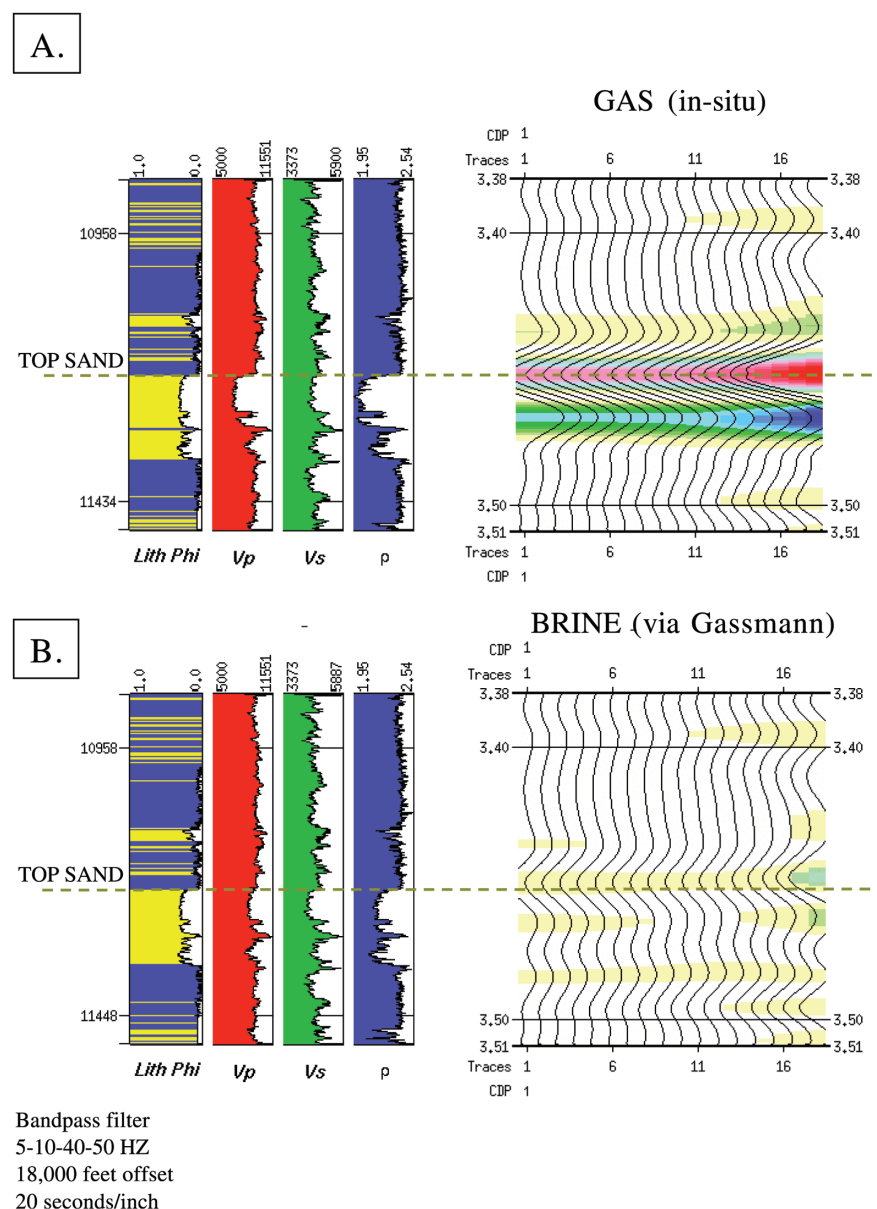


FIG. 8. Offset synthetics for gas and brine over the interval shown in Figure 5. Both models use the same color scale. These models show that even at the seismic bandwidth (5–10–40–50 HZ), a strong AVO response is generated for gas.

REFERENCES

- Alberty, M., 1994, The influence of the borehole environment upon compressional sonic logs, *Trans. Soc. Prof. Well Log Analysts 35th Ann. Logging Symp.*, paper 5.
- Backus, G. E., 1962, Long-wave elastic anisotropy produced by horizontal layering, *J. Geophys. Res.*, **67**, 4427–4440.
- Batzle, M., and Wang, Z., 1992, Seismic properties of pore fluids: *Geophysics*, **57**, 1396–1408.
- Berryman, J. G., 1999, Origin of Gassmann's equations: *Geophysics*, **64**, 1627–1629.
- Berryman, J. G., and Milton, G. W., 1991, Exact results for generalized Gassmann's equation in composite porous media with two constituents: *Geophysics*, **56**, 1950–1960.
- Berryman, J. G., and Wang, H. F., 2000, Elastic wave propagation and attenuation in a double-porosity dual-permeability medium: *Internat. J. Rock Mech. and Min. Sci.*, **37**, 63–78.
- Berge, P. A., 1998, Pore compressibility in rocks, in Thimus, J.-F., Abousleiman, Y., Cheng, A.H.-D., Coussy, O., and Detournay, E., Eds., *Biot Conference on Poromechanics*: Université Catholique de Louvain, 351–356.
- Biot, M. A., 1956, Theory of propagation of elastic waves in a fluid saturated porous solid. I. Low frequency range and II. Higher-frequency range: *Acoust. Soc. Am.*, **28**, 168–191.
- , 1962, Mechanisms of deformation and acoustic propagation in porous media: *J. Appl. Phys.*, **33**, 1482–1498.
- Brie, A., Pampuri, F., Marssala A. F., and Meazza, O., 1995, Shear sonic interpretation in gas-bearing sands; *SPE Ann. Tech. Conf.*, 701–710.
- Brown, R., and Korringer, J., 1975, On the dependence of the elastic properties of a porous rock on the compressibility of the pore fluid: *Geophysics*, **40**, 608–616.
- Budiansky, B., and O'Connell, R. J., 1976, Elastic moduli of a cracked solid: *Internat. J. Solids and Structures*, **12**, 81–97.
- Carmichael, R. S., 1989, Practical handbook of physical properties of rocks and minerals: CRC Press.
- Castagna, J. P., Batzle, M. L., and Kan, T. K., 1993, Rock physics—the link between rock properties and AVO response, in Castagna, J. P., and Backus, M. M., Eds., *Offset-dependent reflectivity—theory and practice of AVO analysis*; *Soc. Expl. Geophys.*, 131–171.

- Castagna, J., and Hooper, J., 2000, A simple method for fitting P-wave velocity versus saturation curves: 70th Ann. Internat. Mtg., Soc. Expl. Geophys., Expanded Abstracts, 1887–1890.
- Castagna, J. P., and Swan, H. W., 1997, Principles of AVO crossplotting: *The Leading Edge*, **4**, 337–342.
- Clark, V. A., Tittman, B. R., and Spencer, T. W., 1980, Effects of volatiles on attenuation and velocity in sedimentary rocks: *J. Geophys. Res.*, **85**, 5190–5198.
- Connolly, P., 1999, Elastic impedance: *The Leading Edge*, **18**, 438–452.
- Danesh, A., 1998, PVT and phase behaviour of petroleum reservoir fluids: Elsevier.
- Eberhart-Phillips, D., Han, D.-H., and Zoback, M. D., 1989, Empirical relationships among seismic velocity, effective pressure, porosity, and clay content in sandstone: *Geophysics*, **54**, 82–89.
- Endres, A. L., and Knight, R., 1989, The effect of microscopic fluid distribution on elastic wave velocities: *The Log Analyst*, Nov-Dec, 437–444.
- Gassmann, F., 1951, Über die Elastizität Poröser Medien: *Vier. der Natur. Gesellschaft in Zürich*, **96**, 1–23.
- Gregory, A. R., 1976, Fluid saturation effects on dynamic elastic properties of sedimentary rocks: *Geophysics*, **41**, 895–921.
- Han, D.-H., Nur, A., and Morgan, D., 1986, Effects of porosity and clay content on wave velocities in sandstones: *Geophysics*, **51**, 2093–2107.
- Hashin, Z., and Shtrikman, S., 1962, A variational approach to the elastic behavior of multiphase materials: *J. Mech. Phys. Solids*, **11**, 127–140.
- Hill, R., 1963, Elastic properties of reinforced solids: Some theoretical principles: *J. Mech. Phys. Solids*, **11**, 357–372.
- Knight, R., and Nolen-Hoeksema, R., 1990, A laboratory study of the dependence of elastic wave velocities on pore scale fluid distributions: *Geophys. Res. Lett.*, **17**, 1529–1532.
- Mavko, G., Mukerji, T., and Dvorkin, J., 1998, *The Rock physics handbook: Tools for seismic analysis in porous media*: Cambridge Univ. Press.
- McCain, W. D., 1990, *The Properties of petroleum fluids*: PennWell Books.
- McLean, M., and Alberty, M., 2001, Dissolved gas in brine: Its impact on fluid substitution: *Trans. Soc. Prof. Well Log Analysts* 42nd Ann. Logging Symp., paper QQ.
- Murphy, W., Reischer A., and Hsu, K., 1993, Modulus decomposition of compressional and shear velocities in sand bodies: *Geophysics*, **58**, 227–239.
- Nur, A., Mavko, G., Dvorkin, J., and Gal, D., 1995, Critical porosity: The key to relating physical properties to porosity in rocks: 65th Ann. Internat. Mtg., Soc. Expl. Geophys., Expanded Abstracts, 878.
- O'Connell, R. J., 1984, A viscoelastic model of anelasticity of fluid saturated porous rocks, in Johnson, D. L., and Sen, P. N., Eds., *Physics and chemistry of porous media: Amer. Inst. Physics*, 166–175.
- Packwood, J. L., and Mavko, G., 1995, Seismic signatures of multi-phase reservoir fluid distribution: Application to reservoir monitoring: 65th Ann. Internat. Mtg., Soc. Expl. Geophys., Expanded Abstracts, 910–913.
- Ramamoorthy, R., and Murphy, W. F., 1998, Fluid identification through dynamic modulus decomposition in carbonate reservoirs: *Trans. Soc. Prof. Well Log Analysts* 39th Ann. Logging Symp., paper Q.
- Raymer, L. L., Hunt, E. R., and Gardner, J. S., 1980, An improved sonic transit time-to-porosity transform: *Trans. Soc. Prof. Well Log Analysts* 21st Ann. Logging Symp.
- Sbar, M. L., 2000, Exploration risk reduction: An AVO analysis in the offshore middle Miocene, central Gulf of Mexico: *The Leading Edge*, **19**, 21–27.
- Shuey, R. T., 1985, A simplification of the Zoeppritz equations: *Geophysics*, **50**, 609–614.
- Sonderegger, C. H., and Rai, C. S., 1993, A new exploration tool: Quantitative core characterization: *Pageoph*, **141**, 249–268.
- Spencer, J. W., Cates M. E., and Thompson, D. D., 1994, Frame moduli of unconsolidated sands and sandstones: *Geophysics*, **59**, 1352–1361.
- Vernik, L., 1998, Acoustic velocity and porosity systematics in siliciclastics: *The Log Analyst*, July-Aug., 27–35.
- Vernik, L., and Fisher, D., 2001, Estimation of net-to-gross from P and S impedance: Part I—Petrophysics: 71st Ann. Internat. Mtg: Soc. Expl. Geophys., Expanded Abstracts, 207–210.
- Walls, J. D., and Carr, M. S., 2001, The use of fluid substitution modeling for correction of mud filtrate invasion in sandstone reservoirs: 71st Ann. Internat. Mtg., Soc. Expl. Geophys., Expanded Abstracts, 385–387.
- Wang, A., 2000, Velocity-density relationships in sedimentary rocks, in Wang, Z., and Nur, A., Eds., *Seismic and acoustic velocities in reservoir rocks, 3: Recent developments*: Soc. Expl. Geophys., 8–23.
- Wang, Z., 2001, Fundamentals of seismic rock physics: *Geophysics*, **66**, 398–412.
- Wang, Z., Wang, H., and Cates, M. E., 2001, Effective elastic properties of clays: *Geophysics*, **66**, 428–440.
- Wyllie, M. R. J., Gergory, A. R., and Gardner, L. W., 1956, Elastic wave velocities in heterogeneous and porous media: *Geophysics*, **23**, 41–70.
- Wyllie, M. R. J., Gergory, A. R., and Gardner, L. W., 1958, An experimental investigation of factors affecting elastic wave velocities in porous media: *Geophysics*, **23**, 459–493.
- Zhu, X., and McMechan, G. A., 1990, Direct estimation of the bulk modulus of the frame in fluid saturated elastic medium by Biot theory: 60th Ann. Internat. Mtg., Soc. Expl. Geophys., Expanded Abstracts, 787–790.